New Insights into the Use of a Rotational Rheometer as Tribometer

Jörg Läuger and Kartik Pondicherry

Anton Paar Germany GmbH, Ostfildern, Germany
Anton Paar GmbH, Graz, Austria

ABSTRACT

The tribometer accessory for a rheometer introduced some years ago has been extended into a tribometer platform. The new features are described in detail and some relevant application examples including Stribeck curves, static friction determination, and wear testing on different materials are discussed and show the wide range of applications.

INTRODUCTION

It is often advantageous to use a model tribometer for gaining experimental tribological data in a fast, reliable and reproducible fashion. Such data offer a tremendous help in the understanding of situations in more complex machines and real life applications. Moreover, simulation techniques can be easily checked by data generated from tribological model systems. A model tribometer requires speed and load control as well as a force or torque measurement to acquire tribological data. An air bearing supported rotational rheometer allows the measurement of the same variables but, concerning speed and torque, in a broader range and with better accuracy compared to a more traditional tribometer. This fact and the intension to perform both speed and torque controlled experiments to measure Stribeck curves as well as the static friction with one single instrument led to the idea to design a tribology attachment turning a commercial available rheometer into a high resolution tribometer based on the ball-on-three-plates principle. In 2006 such a tribology accessory based on a Peltier temperature control was presented[1]. The setup allows the measurements of Stribeck curves over large speed ranges as well as investigations on static friction by applying sliding forces and measure the resulting sliding distances. This tribometer accessory has been used extensively and a number of research papers have been published using the ball-on-three-plate setup by different research groups[2-12].

In the meantime the original ball-on-three-plates setup has been extended into a tribometer platform broadening the application range in numerous directions:

1. A ball-on-three-plate geometry for the use in a convection oven for temperature control widens the temperature range from -150°C up to +600°C.
2. A humidity chamber offers the possibility of simultaneous control of the temperature and the relative humidity in a range of 5% to 95% relative humidity.
3. An additional holder system for the ball-on-three-plate system decreases the lower limit of the load range by a factor of 10 to 0.03N, thus allowing more measurement options, particularly on sensitive soft materials for bio-tribological applications.

4. New geometries such as pins-on-three-plates, ball-on-three-balls (four balls), a larger ball-on-three-plate geometry with larger ball diameter, and holder for O-rings and rolling bearings broaden the application range tremendously.

5. A separate pins-on-disc system, similar to the more traditional pin-on-disc devices, is well suited for example for the use with different surface treated discs. By using different contacts such as flat-on-flat, line-on-flat, and point-on-flat it is possible to vary the contact pressure over a large range with this setup.

6. Measurement techniques which are standard in rheological testing such as oscillatory testing in combination with torque control give new detailed insight, particularly in the behaviour below and at the static or limiting friction. Tribological oscillatory properties such as an elastic friction modulus and a dissipation (loss) friction modulus have been introduces thus offering a possibility to distinguish between elastic and dissipated contributions in tribological contacts around the limiting friction.

The aim of this contribution is to illustrate and to discuss the different new options as well as to present some examples on the use of the model tribometer platform ranging from static friction measurements, Stribeck curves, and wear testing on different materials under various environmental conditions.

TRIBOMETER PLATFORM AND METHODS

In Fig. 1 the ball-on-three-plate geometry with the corresponding Peltier temperature control unit (temperature range: -40°C - +200°C) is shown. The bottom part with the plates sits on a self-centering spring system enabling a movement in x-, y-, and z-direction. The ball has a diameter of 12.7mm (1/2 inch) and the plates are arranged in a 45° angle. With this geometry the speed, torque and normal force ranges lead to the following tribological measuring ranges: Normal load FL: 0.3 - 23N (FN,Tribo); Friction force FF: 0.01 - 44.5N; Sliding speed sv : 10-8 - 1.41m/s. Details of the geometry are depicted in Fig. 2.

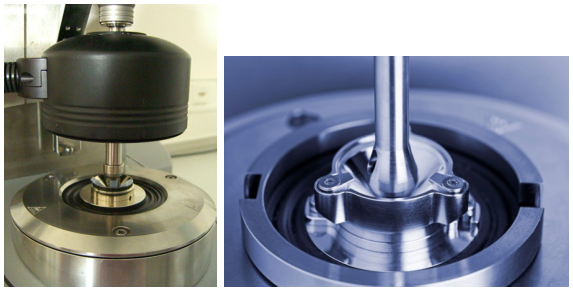

Figure 1. Ball-on-three-plate setup with Peltier temperature control system.

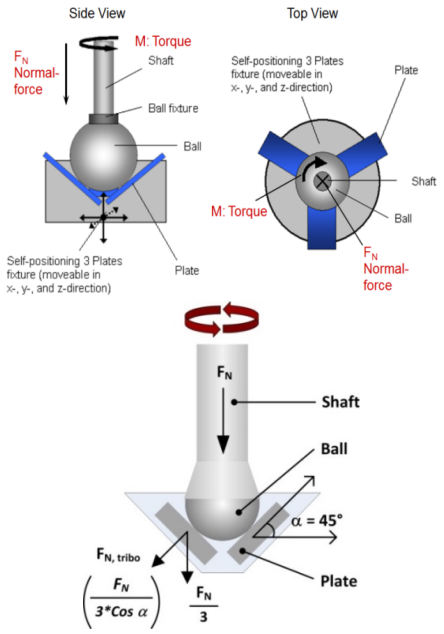

Figure 2. Schematics of the ball-on-three-plates geometries. Top: Side and top view of the geometry. Bottom: tribological load ($F_{N, tribo}$) calculated from the rheometer normal force.

As indicated in Fig. 3, instead of the standard ball-on-three-plate system various different geometries can be used in conjunction with the Peltier controlled environmental system such as for example ball-on-three-pins, or ball-on-three-balls (four-balls). A larger ball extends the

measuring range for the sliding speed by more than a factor of two to 3.33 m/s. Balls are available in different steel alloys, glass and various polymer materials (e.g. POM, PA6.6), whereas plates and pins are additionally available in aluminium (plates), PTFE (plates and pins), and PDMS (pins), respectively. The PDMS pins are used for investigations which mimic soft surfaces as they are prevalent in many bio-tribological applications. The modular design makes it simple to adapt further geometries and to use application specific surfaces for the upper and lower parts of the tribological system. For rolling bearing tests a special holder adapts the bearings to the instrument. With an O-ring holder O-rings can be fixed and tribologically measured.

Figure 3. Left: Different bottom parts for the use with an upper ball, including 3-pins, 3-balls, 3-discs, as well as larger ball for a larger maximum sliding speed. Right: rolling ball bearing holder.

In order to extend the temperature range a bottom geometry holder was designed, which fits into the existing gas convection ovens of the rheometer. A self-centering low friction device for the x- and y- directions in combination with an adjustable spring for the z-direction extends the tribological load range by a factor of 10 towards smaller loads compared to the standard Peltier setup. With the load $F_{N,tribo}$ ranging from 0.03 – 23 N and for an example of a steel ball on steel plates measurements with Hertzian contact pressures from 0.1 up to more than 1 GPa are possible. Similar like in the case of the standard Peltier system, different bottom geometries such as ball-on-three-plates and ball-on-three-pins are possible. The bottom geometry holder fits into tan electrically heated gas convection oven, which, in combination with an additional liquid nitrogen supply, enables a temperature range from -150°C up to +600°C. It also fits into a Peltier controlled gas convection oven, which can be operated in the range of -20°C - +180°C, and which also can be used for providing a humidity control from 5 - 95% relative humidity in a temperature range of 5 - 120°C depending on the relative humidity. In Fig. 4 the various environmental systems based on gas convection are shown.

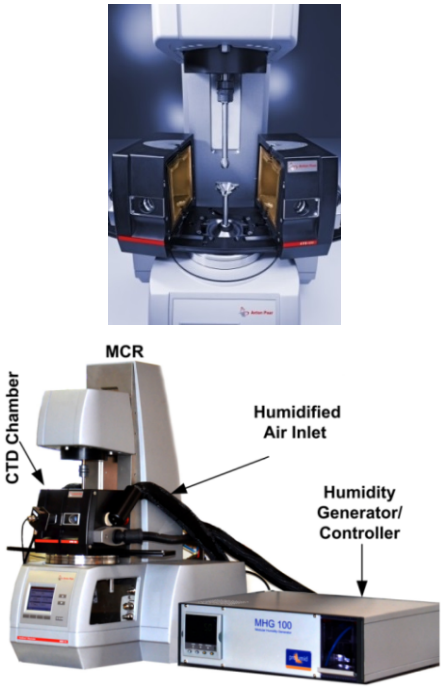

Figure 4. Top: Tribological geometry in an electrical heated gas convection oven (-150°C - +600°C); bottom: Setup for humidity control with rheometer.

Although the rotating ball geometry already simulates many very different applications in a model-tribology approach, for some applications it would be favourable to have pins or balls sliding over a solid surface. For example in rotating ball geometries a liquid sample such as an oil or lubrication grease is pushed through the tribological contact by the rotation ball, whereas in a sliding motion the ball or pins

slide over the liquid sample. Therefore a pins-on-disc setup as depicted in Fig. 5 has been designed. Three pins sit on adjustable springs and are pressed with a load towards the disc surface and a rotated by the rheometer motor. Temperature control is provided by the standard Peltier system in the range of -40°C to +200°C. By using different contacts such as point-on-flat (balls-on-disc), flat-on-flat (pins-on-disc), or line-on-flat (cylinder-on-disc) very different contact areas and therefor different Hertzian contact pressure ranges can be achieved easily. The discs can be changed quickly making this setup especially valuable for investigations on coating surfaces.

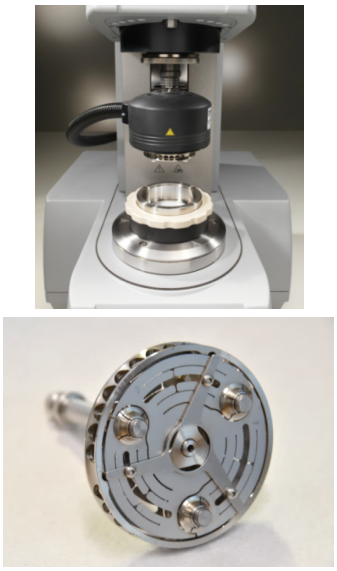

Figure 5. Pins-on-disc setup. Pins, balls, cylinders can be used. Top: Pins-on-Disc on the rheometer with Peltier temperature system; bottom: Upper part of geometry with exchangeable pins.

A standard procedure for rheological investigations on visco-elastic materials are oscillatory tests. In the so-called linear visco-elastic range typically a sinusoidal wave with a pre-selected amplitude and frequency in shear stress (or shear strain) is applied to a sample in a defined geometry and the resulting sinusoidal shear strain (or shear stress) is analyzed with respect to the amplitude of the resulting wave and the phase shift between the two waves. Based on such measurements a storage shear modulus and a loss shear modulus representing the elastic (stored energy) and the viscous contribution (dissipated energy), as well as a complex shear modulus are defined[13]. Similar to this approach friction moduli are introduced as schematically shown in Fig. 6. The friction force F_F and the sliding distance s are the relevant set and response function, i.e. the friction force is set and the sliding distance is measured or vice versa. $\hat{F}_F$ is the amplitude of the friction force in N, $\hat{s}$ is the amplitude of the sliding distance in m, and δ is the phase shift angle.

$G_F' = (\hat{F}_F / \hat{s})\cdot\cos(\delta)$ and $G_F'' = (\hat{F}_F / \hat{s})\cdot\sin(\delta)$ are defined as elastic (stored energy) and as dissipation (loss) friction modulus (dissipated energy), respectively. $|G_F^*| = (G_F'^2 + G_F''^2)^{1/2}$ is the absolute value of the complex friction modulus and $\tan(\delta) = G_F'' / G_F'$ is called the loss factor.

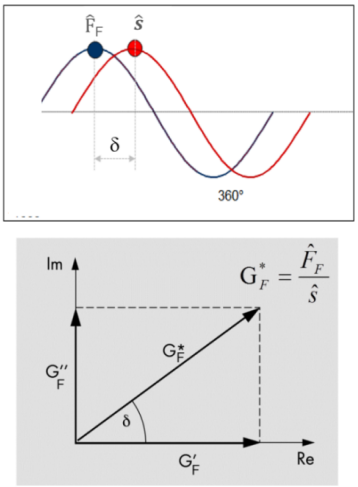

Figure 6. Oscillatory measurements in tribology. Top: set and response wave in frictional force and sliding distance; bottom: complex representation of friction moduli.

The unit of all three moduli is Pa·m, which is intuitive. The unit in rheology where three dimensional shaped samples are

being measured is Pa. In tribology no sample thickness is defined and therefor one dimension is missing and the resulting moduli have a unit of Pa·m.

For measuring static (or limiting friction) behaviour an approach using oscillatory testing is to use a fixed frequency and increase the amplitude of the friction force logarithmically until a significant movement is measured, i.e. the amplitude of the sliding distance is increasing substantially. Such a test is referred to as an amplitude sweep.

TRIBOLOGY OF FUELS

Fuels pose a special case as lubricants. Due to their low viscosity, they are poor film formers. Thus, wear protection and friction modulation is strongly dependent on the surface-active components and other additives in the fuels. The wear-protection and friction-modulating properties of fuels is often evaluated by using a high-frequency reciprocating rig test (HFRR; DIN EN ISO 12156-1). In this test a ball is pressed with a fixed load onto a defined steel plate and moved in a reciprocating manner. As smaller the wear-tracks area on the ball after the test as better the lubricating properties of the fuel are. As an integral quantity is analyzed in the HFRR test, the result can include static, mixed and possibly hydrodynamic friction. It can be difficult to distinguish between different causes for a specific wear behavior in such a test, although this could be valuable information, especially when optimizing components for applications where fuel is the only lubricant.

Four fuels were tested in a ball-on-three-plate geometry with a steel ball and steel plates: diesel, gasoline and two ethanol–gasoline mixtures; 5% ethanol (E5) and 30% ethanol (E30). To investigate fuel lubricity in different friction regimes, Stribeck curves were determined at logarithmically increasing sliding speeds from 0.01 to 1400 mm/s at a load of $F_{N,tribo}$ = 1.5 N (i.e. Hertzian contact pressure = 0.5 GPa). The static friction was determined by oscillatory measurements at a frequency of 1 Hz, where the torque amplitude was increased logarithmically from 0.3 to 10 mNm, while measuring the amplitude of the movement. Further, the wear scars on the balls were evaluated after a sliding distance of 250 m at a constant sliding speed of 47 mm/s.

The results of these tribometric tests are summarized in Fig. 7. Stribeck curves depict the changes in coefficient of friction (COF) relative to the rotational speed. All fuels show a similar COF at high sliding speeds, whereas Diesel has the lowest COF at small and medium sliding speeds. Static friction measurements for all fuels, each averaged over three repeated tests, indicate the lowest static friction value for Diesel followed by gasoline. The ethanol-gasoline mixtures have a significantly larger static friction value. Wear-scar diameters are listed in Table 1 and were compared to the results from the HFFF test. Diesel has the lowest wear-track area, i.e. the best lubricity, while E30 has the largest area, i.e. the poorest lubricity, respectively.

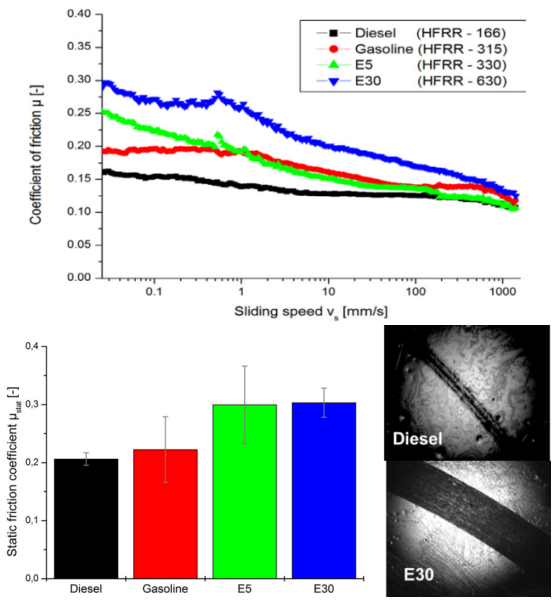

Figure 7. Tribometric tests on fuels: Left: Stribeck cuves (COF as friction of sliding speed); Middle: Results of static friction

tests; Right: Example of wear scars on the ball after wear-test.

The presented results show that a wear-track analysis reveals good correlation with the HFRR test. In addition a more detailed investigation illustrates the benefits of measuring Stribeck curves and determining static friction when characterizing fuel lubricity.

Sample	HFRR	Wear Scar
Diesel	166 µm	125 µm
Gasoline	315 µm	210 µm
E5	330 µm	225 µm
E30	630 µm	320 µm

Table 1. Results from HFRR and wear scar test with ball-on-three-plate geometry.

DEPENDENCE OF THE STATIC FRICTION ON RELATIVE HUMIDITY

In many real life applications the humidity conditions change due to weather or geographical location. Understanding and controlling the humidity dependence of tribological systems can be crucial for an impeccable functioning of many products. As an example model tribosystem consisting of a ball-on-three-plates geometry with a steel ball and plates made of Polyoxymethylene (POM) and Polyamide 6.6 (PA6.6) have been investigated at various levels of the relative humidity in the humidity chamber described previously. In order to determine the static friction behavior the torque has been ramped up logarithmically from 0.02 up to 50 mNm, representing a friction force range from 0.0045 up to 11 N. The load in a pre-test holding step for 15 min as well as in the actual test was $F_{N,tribo}$ = 5 N. The data presented in Fig. 8 reveal a strong dependence of the braking torque, i.e. the static friction, on the relative humidity. As higher the humidity as larger the static friction for both polymer samples is. PA6.6 shows a stronger influence of the relative humidity compared to POM.

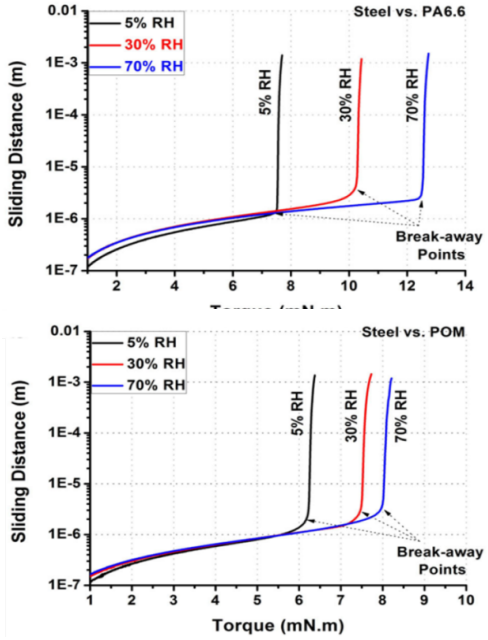

Figure 8. Sliding distance as a function of torque for three levels of relative humidity (5%, 30%, 70%). Top: Steel ball on PA6.6 plates; Bottom: Steel ball on POM plates.

OSCILLATORY TESTING

In order to test the concept of oscillatory testing and the evaluation of friction moduli, dry contacts between a steel ball and POM and PA6.6 plates have been measured in a ball-on-three-plate setup: The geometry for the convection oven has been selected since it allows smaller tribological loads. For the tests depicted in Fig. 9 a load of $F_{N,tribo}$ = 1 N has been employed.

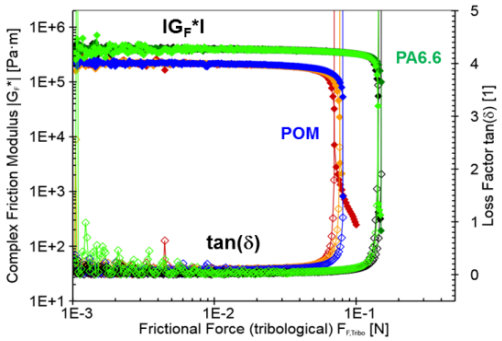

Figure 9. (continued)

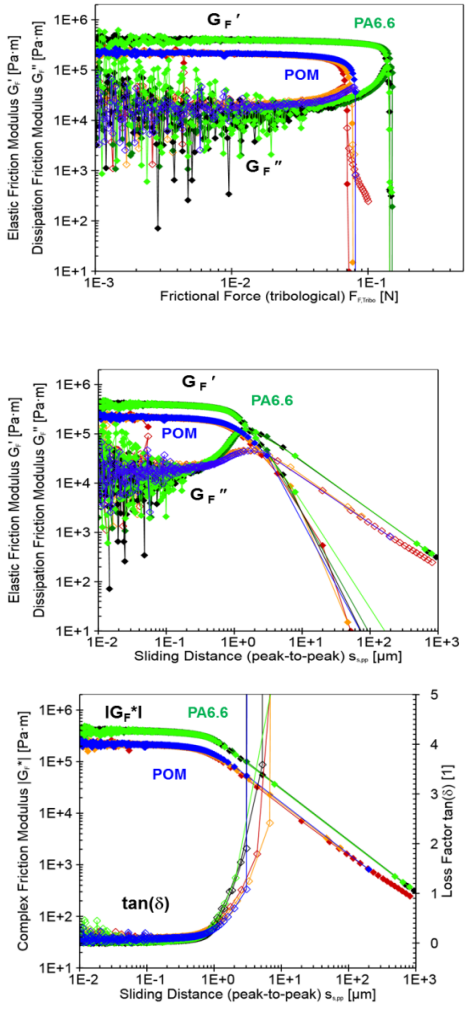

Figure 9. Frictional force sweeps at 1Hz and 1 N load. Three repeats for POM and the PA6.6. Elastic and dissipation friction moduli (left) and complex friction modulus and loss factor (right) as a function of the friction force (top) of the amplitude of the sliding distance (bottom).

After a holding period of 90 s at this load an oscillatory sweeps in friction force with a amplitude varying from 0.001 up to 10 N with a fixed frequency of 1 Hz have been performed. Three repeats for each sample show a good reproducibility.

At small forces both samples show a linear elastic modulus, the dissipation modulus is very small and therefor the signals are quite noisy. Since the dissipation modulus is small at small force amplitudes the complex modulus is similar to the elastic modulus, whereas the loss factor is close to zero. The system is rather stiff and does not absorb much energy. PA6.6. has a higher elastic modulus indicating a stiffer contact compared to POM. The friction force at which the elastic modulus decreases strongly is larger for PA6.6, i.e. the steel-PA6.6 contact has a larger static friction compared to the steel-POM contact. On the other side, the drop in the moduli occurs for both systems at similar sliding distances indicating, that the two systems can absorb different forces, but can be deformed by the same amount, before real sliding happens. The increase in the dissipation modulus before the elastic modulus drops can be related to an energy dissipation do to local slip by at the steel polymer interface. PA6.6 exhibit a larger peak in the dissipation modulus compared to POM. The rate of decrease of the elastic modulus is an indication of the nature of the static-kinematic transition. A slower decrease favours a sliding away transition in contrast to a more brittle fracture. The steel-POM system shows a slightly slower decrease compared to the steel-PA6.6 system. Such oscillatory measurements are a valuable tool to investigate tribo-contacts at around the point of the limiting friction on different time scales and loads.

CONCLUSIONS

A tribometer platform based on a rotational rheometer offers a lot of measurement options on tribological model systems, many of them not available on other instruments. The main advantages of the use of a rotational rheometer are its sensitive rotational motor, which operates in a speed range covering nine decades and in a torque range of eight decades as well as the precise control system of temperature and humidity. Stribeck curves, static friction determination, and wear testing on materials as different as lubricants, polymers, and

food under various different environmental conditions show the wide range of applications covered by such a type of tribometer.

REFERENCES

1. Heyer P. and Läuger J. (2009) "Correlation between friction and flow of lubricant greases in a new tribometer device" *Lubrication Science*, **21**, 253-268

2. Bombard A.J.F. and de Vicente J. (2012) "Thin-Film Rheology and Tribology of Magnetorheological Fluids in Isoviscous-EHL Contacts" *Tribol. Lett.*, **47**,149–162

3. Bombard A.J.F. and de Vicente J. (2012) "Boundary lubrication of magneto-rheological fluids in PTFE/steel point contacts" *Wear*, **296**, 484–490

4. Boettcher K.,Grumbein S.,Winkler U.,Nachtsheim J. and Lieleg O. (2014) "Adapting a commercial shear rheometer for applications in cartilage research" *Rev. Sci. Instrum.*, **85**, 093903

5. Schlüter B., Mülhaupt R. and Kailer A. (2014) "Synthesis and Tribological Characterization of Stable Dispersions of Thermally Reduced Graphite Oxide" *Tribol Lett.*, **53**, 353–363

6. Kienle S., Boettcher K., Wiegleb L., Urban J., Burgkart R., Lieleg O, Hugel T. (2015) "Comparison of friction and wear of articular cartilage on different length scales" *Journal of Biomechanics*, **48**, 3052–3058

7. Dold Ch. Amann T. and Kailer A (2015) "Influence of electric potentials on friction of sliding contacts lubricated by an ionic liquid" *Phys. Chem. Chem. Phys.*, **17**, 10339-10342

8. Crouzier T., Boettcher K., Geonnotti A.R., Kavanaugh N.L., Hirsch J.B., Ribbeck K. and Lieleg O. (2015) "Modulating Mucin Hydration and Lubrication by Deglycosylation and Polyethylene Glycol Binding" *Adv. Mater. Interfaces*, 1500308

9. Bombard A.J.F., Gonçalves F.R., Shahrivar K., Ortiz A.L. and deVicente J. (2015) "Tribological behavior of ionic liquid-based magnetorheological fluids in steel and polymeric point contacts" *Tribology International*, **81**, 309–320

10. Gilardi R. (2016) "Tribology of Graphite-Filled Polystyrene" *Lubricants* **4**, 20-27

11. Amann T., Kailer A., Beyer-Faiß S., Stehr W. and Metzger B. (2016) "Development of sintered bearings with minimal friction losses and maximum life time using infiltrated liquid crystalline lubricants" *Tribology International* **98**, 282–291

12. Gallego R., Cidade T, Sánchez R., Valencia C, Franco J.M. (2016) "Tribological behavior of novel chemically modified biopolymer-thickened lubricating greases investigated in a steel–steel rotating ball-on-three plates tribology cell" *Tribology International* **94**, 652–660

13. Mezger, Th.G. (2014) "The Rheology Handbook", 4th Edition, Vincentz Network, Hannover